濟州大學校 尖端技術硏究所 論文集, 第18卷, pp.57-68, 2007. 12
Cheju Nat'l Univ. Res. Inst. Adv. Tech. Jour., Vol.18, pp.57-68, 2007. 12

Effective Application of Sonar Data for SLAM

Se-Jin Lee* · Jong-Hwan Lim**

ABSTRACT

This paper shows how effectively sonar data can be worked with approaches suggested for the indoor *SLAM* (Simultaneous Localization And Mapping). A sonar sensor occasionally provides wrong distance range due to the wide beam width and the specular reflection phenomenon. To overcome weak points enough to use for the *SLAM*, several approaches are proposed. First, distance ranges acquired from the same object have been stored by using the *FPA* (Footprint-association) model, which associates two sonar footprints into a hypothesized circle frame. Using the Least Squares method, a line feature is extracted from the data stored through the *FPA* model. However phantom features are sometimes generated due to the uncertainties of a sonar sensor. The feature evaluation model is applied to reduce phantom features, which associates the extracted feature with the weighted average probability of grids that are located within the area under the feature uncertainty. By using raw sonar data together with the extracted features as observations, the visibility for landmarks can be improved, and the *SLAM* performance can be stabilized. Additionally, the *SP* (Symmetries and Perturbations) model, a representation of uncertain geometric information that combines the probability theory and the theory of symmetries, is applied in this paper. The proposed methods have been tested in a real home environment with a mobile robot.

Key Words : Feature Extraction and Evaluation, SLAM, Sonar Observations, Ultrasonic Sensor

Ⅰ. Introduction

Successful *SLAM* as well as path planning and obstacle avoidance is required before anything else for autonomous navigation of a mobile robot. Many researchers have used high price and performance sensors such as camera and laser scanner to achieve better *SLAM* results. Siegwart et al. introduced the concept of the relative features and executed *SLAM* with a laser scanner[1]. Tardos et al. suggested the solution of a representation problem of features by developing and applying *SP* model[2]. Davison et al. have done the bearing-only *SLAM* with a single camera[3]. The *SLAM* with a sonar sensor is also quite worthy of research from the commercial point of view

* Dept. of Mechanical Engineering, POSTECH.
** Faculty of Mechanical, Energy & System Eng., Res. Inst. of Adv. Tech., Cheju National University.

that efficient *SLAM* with only cheap sensors is important.

Tardos et al. extracted features through the *Hough transform* with sonar data of 24 *Polaroid* sensors and developed the local map joining and loop closing algorithm for *SLAM*[4]. Christensen et al. developed the *TBF* (Triangulation-based fusion) algorithm for extracting point features and tracked a robot pose with pre-recorded reference maps of landmarks[5]. Kleeman et al. have realized the landmark classification and *SLAM* by making the advanced sonar ring with 48 *Polaroid* sensors[6]. However, researches mentioned above used high performance *Polaroid* sensors, and their methods were not verified in a complicated place such as home-like environment. Moreover, they did not confirm the *SLAM* stability for real environment or long time operation.

This paper shows how effectively sonar data of a piezo type sensor can be worked with approaches suggested for the indoor *SLAM*. A sonar sensor occasionally provides wrong distance range due to the wide beam width and the specular reflection phenomenon. Chapter II introduces the *FPA* model that associates two sonar footprints to overcome defects of sonar. The process of the feature extraction by using the Least Squares method is also given. However, phantom features are sometimes generated due to the uncertainties of a sonar sensor. The feature evaluation model that reduces phantom features is explained in chapter III, which associates the extracted feature with the weighted average probability of grids that are located within the area under the feature uncertainty. By using raw sonar data together with the extracted features as observations, the visibility for landmarks can be improved, and the *SLAM* performance can be stabilized. The *SP* model, a representation of uncertain geometric information that combines the probability theory and the theory of symmetries, is given in this chapter. Chapter IV shows the framework of *SLAM* with the flowchart. The results of the proposed methods tested in a real home environment with a mobile robot are reported in chapter V. Finally conclusions are drawn in chapter VI.

II. Feature Extraction

2.1 Ultrasonic Sensor

Some researchers have put a great deal of effort into building good quality sonar maps[7]-[12]. While some successful results have been reported, most of the results were very poor because ultrasonic sensors have considerable angular uncertainty due to their wide beam aperture, and suffer from the specular reflection effect[10]-[12].

Ultrasonic sensors return a radial measure of distance to the nearest object within their range of detection. However, they frequently fail to detect the nearest object. There are two possible explanations for this[11]-[12]. First, the surface of an object may produce an echo amplitude that is too small to be detected by the receiver. Second, the echo pulse may be reflected away by a surface that is not perpendicular to the transducer axis. Since the surfaces of most real-world objects can be considered specular for ultrasonic sensors, this effect is almost always observed when the incidence angle is greater than half the beam aperture[10].

The *RCD* method is one simple and powerful

means of reducing both the specular reflection effect and angular uncertainty[13]. However, these methods can be hardly used when data are scanned sparsely because neighboring sets of these data have few associations. Single rotating sonar is usually applied to get densely scanned data, but it is not adequate for actual applications because it has a slow data acquisition speed. In addition, it requires a robot to stop when acquiring scanned data.

In this study, a sonar ring was used to get data quickly while a robot was in motion. 12 piezo-type sensors made by *HAGISONIC* were mounted on the sonar ring at a regular interval of 30° that is identical to the effective beam aperture. As mentioned above, sparsely scanned data do not allow using the existing methods of rejecting the incorrect data or those of reducing the angular uncertainty.

2.2 FootPrint-Association Model

The *FPA* model allows determination of whether two sonar footprints are associated with a line, a point, or an arc. Sonar footprints that correspond to a plane or a cylinder should all be tangential to that plane or cylinder, while sonar footprints that correspond to a corner or an edge should all intersect at a corner or edge point[13].

The *FPA* model basically estimates the possibility that two sets of sonar data originate from the same feature. In Fig. 1, we can define two circles centered at sensor locations with radii equal to footprint range values, z_1 and z_2, and define the effective sonar beam aperture as each footprint's constraint angle, represented by the shaded fan shape. We can define a local coordinate system, centered at sensor location 1 (point O in Fig. 1), with sensor location 2 (point B in Fig. 1) on the positive X-axis at position $x=d$, where d is the distance between the two sensor locations. The *FPA* model assumes that if any two sets of range data, z_1 and z_2, originate from the same object, a hypothesized feature should define the third circle, which is tangential to the two circles defined by the footprints [13]. The general problem is, therefore, to find radius R of the third circle that defines the hypothesized feature.

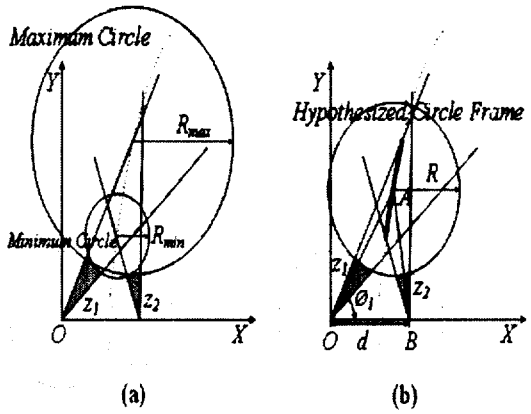

Fig. 1. Hypothesized circles that are tangential to the two circles defined by the footprints: (a) possible range of radii for the hypothesized circles without considering angle constraints, and (b) trace of virtual circle centers that satisfies the angle constraints.

Let ϕ be the bearing from the original of the local coordinate system to the center of a hypothesized circle. We can get ϕ_1 using the law of cosines such as Eq. (1):

$$\phi_1 = \cos^{-1}\left(\frac{(z_1+R)^2-(z_2+R)^2+d^2}{2d(z_1+R)}\right) \quad (1)$$

Unfortunately, we cannot uniquely determine the third circle because both R and ϕ_1 are unknowns. Leonard developed very simple

method to determine the third circle[13]. That is, he found ϕ_1 by taking the limit as $R \rightarrow infinite$ and $R \rightarrow 0$ respectively. As a result, the method can only be applied in the special case of line and point targets. We generalized the method by considering that bearing ϕ for each sensor footprint must simultaneously satisfy the angle constraint defined as an effective beam aperture. This fact makes it possible to calculate the range of bearing, i.e., ϕ_{min} and ϕ_{max}, and the corresponding R_{min} and R_{max}. The bold solid line segment in Fig. 1, defined as the center-line, represents possible center locations of the hypothesized circles with radii between R_{min} and R_{max}.

It is possible to determine the bearing of a hypothesized circle uniquely for some special cases. If R_{min} is very large or approaching infinity, the two footprints are clustered into a line feature. In contrast, if R_{max} is very small or approaching zero, the footprints are clustered into a point. Otherwise, the footprints are clustered into an arc feature. In this paper, only type of line feature among them is used in *SLAM*.

2.3 Feature Extraction through Least Squares

Given the large amount of spurious data coming from specular reflections and sonar artifacts, classical robust techniques such as *RANSAC*[14] or the *Hough transform*[4] seem very appropriate. However, because most of the sonar readings that correspond to the same feature are clustered together by using the *FPA* model in this paper, the information of a line feature can be extracted from each cluster directly by using the *Least Squares* fitting.

The parameters that characterize a line feature are the middle point, the inclined angle, the length, and the visible direction of the line. The visible direction of a line feature, defined as normal direction of the line, represents which side of the line is visible. The visible direction of a line feature is very useful information for the data association in the *SLAM*. Details on the feature extraction are given in [15].

III. Feature Evaluation Method Based on Occpuancy Probability of Grids

Almost all the line feature can be generated at the position of real objects by using the *FPA* filtering and the *LS* fitting. However, there can be unexpected features around a moving people or a complex environment due to wide beam width and specularity of sonar sensors. In this paper, the feature evaluation method is developed based on the probabilistic association using the occupancy probabilities of grids in order to minimize phantom features. For this association, the occupancy probability of grids is necessary to associate the extracted feature with the weighted average probability of the grids within the area of position uncertainty of the feature.

3.1 Grid Mapping

Bayesian probability map is composed of many grids that represent the robot's workspace, and each grid has an occupancy probability of an object. The grids within the sonar footprint, that are to be updated, are rearranged according to the distance from the transducer location. These grids are divided into two regions. One is defined as an empty

region and the other is an occupied region. The occupancy probability for the grid in the empty region should go down, while that in the occupied region should go up. An updating quantity of the occupancy probability is determined by using *Bayes* conditional probability theory according to the distance or angle of the grid from the sensor[9].

Bayesian model can supports a sound theoretical basis of a probability map. In the real application, however, it has a critical problem that seriously deteriorates the quality of the resulting map[12]. That is, the *Bayesian* model does not consider the specular reflection and the multi-path effects that frequently return incorrect range data. To solve this problem, Lim et al. developed a mapping model with ability to detect an occurrence of the specular reflection effect by evaluating the orientation probability in each grid[11]-[12]. In this model, the orientation probability is updated by using the specular reflection effect conversely. As the information is accumulated, the probability of the orientation corresponding to real object surface is continuously increased, while those of the rest orientations will be decreased. An occurring possibility of the specular reflection and the multi-path effects for each sonar range data can be probabilistically considered by using the orientation pro-F babilities. It has been shown that the orientation model can construct a good quality map despite of the specular reflection effect [11]-[12].

3.2 Probabilistic Association for Feature Evaluation

The approach for the reliability evaluation of a feature is based on the occupancy probabilities of the grid map that is built using the hybrid map-building model stated above. This approach can minimize phantom features and maintain dynamic features by using only sparse sonar data. This association is to associate the extracted feature with the weighted average probability of the grids that are located within the area of position uncertainty of the feature as shown in Fig. 2. The formula for the weighted average of the occupancy probability is written as [16]:

$$a=\frac{\sum_{i=0}^{N} P_{O_i}(x,y)P_i(x,y)}{\sum_{i=0}^{N} P_i(x,y)} \qquad (2)$$

where a is the weighted average of the probabilities of grids in the area of feature position uncertainty, N is the number of grids in the ellipse of the position uncertainty. P_{Oi} is the occupancy probability of ith grid, and P_i is the probability of the Gaussian distribution of i_{th} grid.

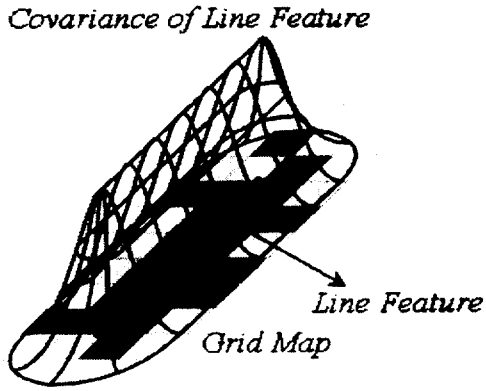

Fig. 2 Ellipse of uncertainty for a line feature. The weighted average of the occupancy probability is found using grids in the area of feature position uncertainty.

IV. SLAM

The simultaneous localization and mapping (*SLAM*) problem asks if it is possible for a mobile robot to be placed at an unknown location in an unknown environment and for the robot to incrementally build a consistent map of this environment while simultaneously determining its location within this map. A solution to the *SLAM* problem has been seen as a "holy grail" for the mobile robotics community as it would provide the means to make a robot truly autonomous[17].

4.1 SP Model

The line feature is too hard to be managed as updating the state in the *EKF* process. For example, if we represent a wall as an edge in 2D, a small uncertainty in the wall orientation gives rise to a very big variance for the perpendicular distance to the origin if the wall is far away from the origin. Therefore this paper applied *SP* model, a representation of uncertain geometric information that combines the use of probability theory to represent the imprecision in the location of a geometric element, and applied the theory of symmetries to represent the partiality due to characteristics of each type of geometric element [2].

The *SP* model represents the information about the location of a geometric element F by a quadruple:

$$L_{WF}=(\hat{x}_{WF}, \hat{P}_F, C_F, B_F) \tag{3}$$

which called the uncertain location of the geometric element F, where:

$$\begin{aligned} x_{WF} &= \hat{x}_{WF} \oplus B_F^T p_F \\ \hat{P}_F &= E[p_F] \\ C_F &= E[(p_F-\hat{p}_F)(p_F-\hat{p}_F)^T] \end{aligned} \tag{4}$$

B_F is the binding matrix of the geometric element, transformation $\hat{x}_{WF}$ is an estimation taken as base for perturbations, $\hat{p}_{WF}$ is the estimated value of the perturbation vector, and C_F its covariance.

The perturbation vector of the *SP* map p^W and its covariance matrix C^W are estimated at time k from the constraints introduced by the matching between local observations acquired at time k and previously available knowledge up to time $k-1$. The general linearized measurement equation can be written as:

$$\begin{aligned} z_{k,m} &= H_{k,m} p_k^W + \nu_{k,m} \\ &; \nu_{k,m} \sim N(0, G_{k,m} S_{k,m} G_{k,m}^T) \end{aligned} \tag{5}$$

Thus, the estimation equation, derived from the classical *EKF* formulation, for the perturbation vector of the *SP* map becomes:

$$\begin{aligned} \hat{p}^{W_{k,m}} &= \hat{p}_{k,m-1}^W + K_{k,m}(z_{k,m} - H_{k,m}\hat{p}_{k,m-1}^W) \\ &= \hat{p}_{k,m-1}^W - K_{k,m} h_m \end{aligned} \tag{6}$$

Similarly, for the covariance matrix of the *SP* map we have:

$$C_{k,m}^W = (I - K_{k,m} H_{k,m}) C_{k,m-1}^W \tag{7}$$

where the filter gain $K_{k,m}$ is calculated by:

$$\begin{aligned} K_{k,m} &= C_{k,m-1}^W H_{k,m}^T \\ &\cdot (H_{k,m} C_{k,m-1}^W H_{k,m}^T + G_{k,m} S_{k,m} G_{k,m}^T)^{-1} \end{aligned} \tag{8}$$

Precision of the results obtained by the application of suboptimal estimation techniques,

based on the *EKF*, to the estimation of a state vector and its covariance matrix is highly influenced by the linearization performed on the non-linear measurement equations relating the state vector with a set of partial observations of its structure. To keep consistency and to avoid biases in the estimation, linearization is accomplished after each observation is integrated into the state vector, thus obtaining a centered state vector p^W. The centered estimated location vector is computed as:

$$(\hat{x}^W)' = \begin{bmatrix} \hat{x}'_{WR} \\ \hat{x}'_{WF} \end{bmatrix} = \begin{bmatrix} \hat{x}_{WR} \oplus \hat{d}_R \\ \hat{x}_{WF} \oplus B_F^T \hat{p}_F \end{bmatrix}. \quad (9)$$

Its perturbation vector becomes the null vector:

$$(\hat{p}^W)' = 0. \quad (10)$$

Its covariance matrix is computed by:

$$(C^W)' = Q^W C^W (Q^W)^T \quad (11)$$

where matix Q^W obtained as:

$$Q^W = \begin{pmatrix} B_R J_{2\oplus}^{-1}\{d_R, 0\} B_R^T & 0 \\ 0 & B_F J_{2\oplus}^{-1}\{B_F^T \hat{p}_F, 0\} B_F^T \end{pmatrix} \quad (12)$$

4.2 Observations

Actual observations of the surroundings by using external sensors are very important to update the full state of the map. Therefore It is not too much to say that the performance of *SLAM* is dependent on the ability of observation of the sensors. A laser scanner and a vision sensor are very good for the *SLAM* because they can give good quality of information enough to use localization even from a single position. However ultrasonic data of a fixed sensor ring from a single point cannot reflect well the shape of the environment at that moment due to wide beam width and the specular reflection. For this reason, most researches who used sonar sensors for the *SLAM* have tried to extract features from accumulated range data. These features were used as the targets of observations in the *EKF* updating step. However, these features would not assure the generations of rich observations for the innovation step in *EKF* because the visibility of the features for sonar sensors is considerably low when compared with the other sensor.

In this paper, we improved the visibility of landmarks by using raw sonar data as observations as well as the extracted features in the *SLAM* updating step. To use raw data as observations, it is necessary to search which landmark is associated with the raw data through the data association. As shown in Fig. 3(a), we can infer a virtual feature using each set of sonar data from the geometric relations among the sonar data, robot pose, and the associated landmark. However, while the feature can give information on both the angle and (x, y) pose, raw sonar data can give information on only x and y poses because the robot's heading cannot be determined uniquely due to the angular uncertainty of the sensors as shown in Fig. 3(b). Even if the angle pose cannot be updated from raw sonar data, the consistency of the *SLAM* is considerably improved when the extracted features and raw sonar data are used together as observations.

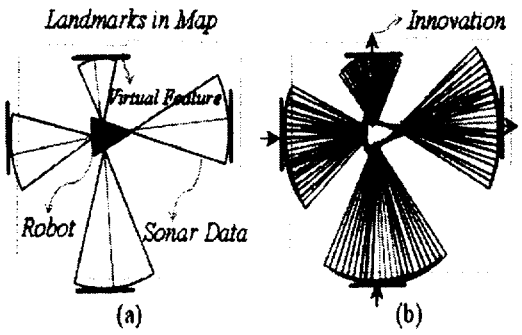

Fig. 3. (a) The virtual features from sets of raw sonar data for the data association of landmarks, (b) Variation of robot's heading due to wide beam width of the sonar sensors.

4.3 Map Management

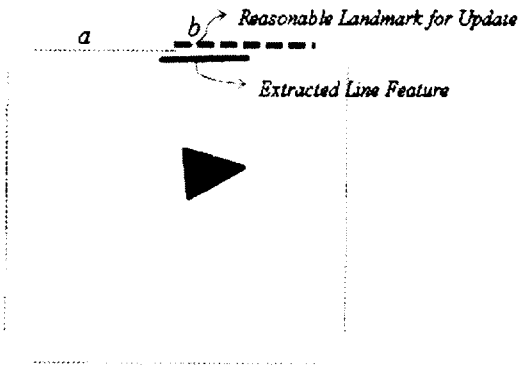

Fig. 4. Removal of temporal features through the occlusion test.

In this paper, the simple map management was applied such as a removal of a short line feature and an occlusion test. The removal of a short line is based on the lapse of time. That is, the line feature is removed if the length of the line is no longer extended till a given lapse of time has passed. Fig. 4 shows a short and newly extracted line feature occludes the other line feature and they are very close to each other. In this case, though the short line is much closer to the robot, it is reasonable to remove the short line because it is less reliable than the long and old one. This can be done by occlusion test, and can keep the map in high reliability. Moreover, the occlusion test is very useful for the *SLAM* in that this makes it possible to avoid the ambiguous data association with more than tow nearby features.

4.4 Framework of SLAM

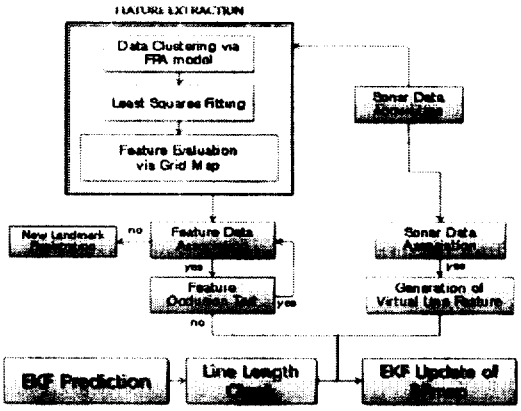

Fig. 5. Flowchart of *SLAM* based on a *SP* map.

Fig. 5 shows the flowchart of the sonar *SLAM* based on a *SP* map. Two kinds of the observations are applied to update the state of the *SP* map, the extracted features through *FPA* model and the raw sonar data themselves. Sets of sonar data that support the same object are clustered together through the *FPA* model, and then the line features are extracted from the clusters by using the *Least Squares* fitting method. The reliability of the extracted line feature is evaluated by the grid association. Finally, the evaluated line feature is used as landmarks in the update step of the *EKF* through the data association and the occlusion test.

The raw sonar data as second observations are associated with environmental map, so that

they make virtual features that are used as the landmarks for *EKF* step. The *EKF* step updates the full states of the *SLAM* by using the *SP* model that combines the use of probability theory and the theory of symmetries to represent uncertain geometric information.

V. Experimental Results

The data clustering by the *FPA* model, the feature evaluation by the grid probabilities, and the *SLAM* stated above have been implemented and tested in a real home environment with a real robot. We used the Pioneer *3DX robot* with a ring of 12 *HAGISONIC* sonar sensors. The transitional and rotation speeds of the robot were approximately 0.2m/s and 15deg/s respectively. In order to test the performance of the data clustering and the feature evaluation, the robot was run followed the guided trajectory in 4.3m×3.6m home-like experiment that is composed of sofas, table, clothes chest, bookshelf, and fire extinguishers.

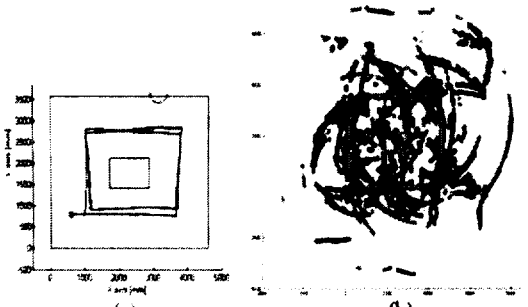

Fig. 6. (a) Experimental environment and robot's path. (b) Scanned raw data and filtered data from the *FPA* model.

In Fig. 6(b), the circles represent scanned raw sonar data during the robot's exploration. As shown in Fig. 6(a), the total trajectory of the robot was about 19.2m, and the traveling time was approximately 2.5 minutes. During the robot's motion, the sonar ring acquired range data with frequencies of 10Hz. In Fig. 6(b), small asterisks (red color) represent filtered sonar data through the *FPA* model. As shown in Fig. 6(b), raw sonar data are scattered due to the wide beam aperture and the specular reflection effect. However, most of the filtered data are located around the position of real objects.

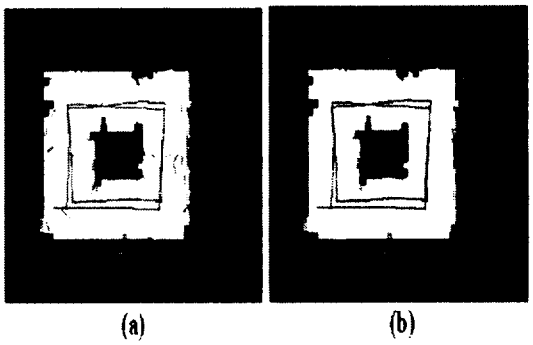

Fig. 7. Occupancy grid map and discrete features. (a) Before applying the probabilistic association. (b) After applying the probabilistic association.

Fig. 7 shows the probabilistic grid map generated from the filtered sonar data using *FPA* model, and the size of a grid is 15 cm×15 cm. Line features were extracted and saved from the data clusters for every 50 cm movement. The probabilistic association was also executed with average frequency of 0.1 Hz. Fig. 7(a) shows all extracted features by *LS* fitting before applying the probabilistic association, and Fig. 7(b) shows the features evaluated by the probabilistic association using the grid map. Although some phantom features are appeared at the free space due to moving people and

wide beam width and specularity of sonar in Fig. 7(a), they were removed clearly by applying the probabilistic association as shown in Fig. 7(b).

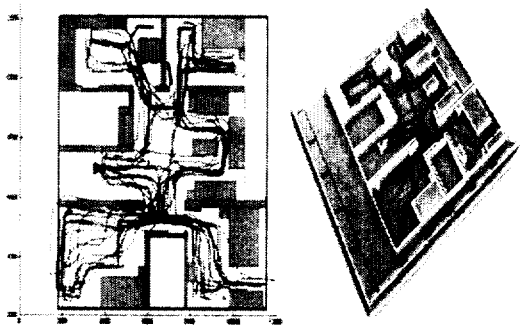

Fig. 8. Odometry and estimated trajectories in a real home environment.

Another experiment for testing the performance of the *SLAM* was carried out in a 10m × 10m guest house at *POSTECH*. The total trajectory of the robot was about 305.99m, and the total traveling time was about 40 minutes with an average speed of 20 cm/s. During the robot's motion, the sonar ring acquired range data with frequencies of 4Hz. Fig. 8 shows the experimental environment. In the figure, the blue and red lines represent the odometric and estimated trajectories respectively.

Fig. 9 shows the final feature map of the experimental environment, which composed of 52 line features. One can see that almost all the boundaries of true objects are reconstructed as line features (blue lines). Position errors of the robot were bounded within a reasonable range, so that the proposed *SLAM* can be applied to practical navigation of mobile robot.

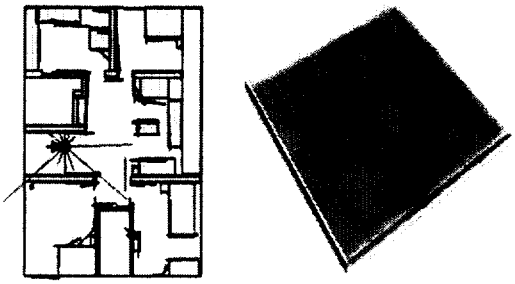

Fig. 9. Result of feature map.

VI. Conclusion

This paper has presented new approaches for *SLAM*, and shown how effectively sparsely scanned sonar data can be used for the indoor *SLAM*. Sets of sonar data acquired from the same object have been clustered by using the *FPA* (Footprint-association) model, which associates two sonar footprints into a hypothesized circle frame. Line features were, then, extracted from the stored clusters through the *Least Squares* method.

The feature evaluation model was applied to reduce phantom features, which associates the extracted feature with the weighted average probability of grids that are located within the area under the feature uncertainty. By using raw sonar data together with the extracted features as observations, we found the visibility for landmarks can be improved, and the *SLAM* performance can be stabilized.

Additionally, the *SP* (Symmetries and Perturbations) model, a representation of uncertain geometric information that combines the probability theory and the theory of symmetries, is applied in this paper. The experimental results have shown that the performance of the proposed *SLAM* is quite good enough to apply it

to a practical indoor navigation of a mobile robot with only sparsely scanned sonar data.

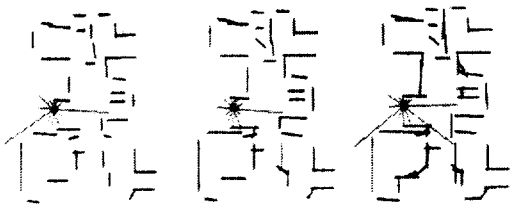

(a) (b) (c)

Fig. 10. Results of maps after completing (a) one loop, (b) two loops, and (c) three loops.

However, as shown in Fig. 10, phantom features tend to appeared over time. It is not awkward when considering its wide beam width and specularity of a sonar sensor. Therefore, an algorithm for reducing the unexpected features should be developed in the future.

References

[1] Kai O. Arras, Jose A. Castellanos, Martin Schilt, and Roland Siegwart, 2003, "Feature-based multi-hypothesis localization and tracking using geometric constraints," Robotics and Autonomous Systems, 1056, pp. 1-13.

[2] Jose A. Castellanos and Juan D. Tardos, 1999, "Mobile Robot Localization and Map Building : A Multisensor Fusion Approach," Kluwer Academic Publishers.

[3] A. J. Davison, 2003, "Real-time simultaneous localization and mapping with a single camera," IEEE Intl. Conf. on Computer Vision, vol. 2, pp. 1403-1410.

[4] J. D. Tardos, Jose Neira, P. M. Newman, and J. J. Leonard, 2002, "Robust Mapping and Localization in Indoor Environments Using Sonar Data," The Intl. Journal of Robotics Research, vol. 21, no. 4, pp. 311-330.

[5] O. Wijk, H. I. Christensen, 2000, "Triangulation-based fusion of sonar data with application in robot pose tracking", IEEE Trans. On Robotics and Automation, vol. 16, no. 6, pp. 740-752.

[6] S. Fazli and L. Kleeman, 2006, "Simultaneous Landmark Classification, Localisation and Map Building for an Advanced Sonar Ring", Accepted for publication in Robotica.

[7] J. L. Crowley, 1985, "Navigation for an intelligent mobile robot", IEEE Journal of Robotics and Automation, RA-1(1), pp. 31-41.

[8] A. Elfes and H. P. Moravec, 1985, "High resolution maps from wide angle sonar," IEEE Intl. Conf. on Robotics and Automation, pp. 116-121.

[9] D. W. Cho, 1990, "Certainty grid representation for robot navigation by a Bayesian method", Robotica, vol. 8, pp. 159-165.

[10] J. H. Lim, 1994, "Map construction, exploration, and position estimation for an autonomous mobile robot using sonar sensors", PhD dissertation, Pohang Institute of Science and Technology, Korea.

[11] J. H. Lim and D. W. Cho, 1994, "Specular reflection probability in the certainty grid representation," Trans. Of the ASME, vol. 116, pp. 512-520.

[12] J. H. Lim and D. W. Cho, 1996, "Multi-path Bayesian map construction model from sonar data," Robotica, vol. 14, pp. 527-540.

[13] J. J. Leonard, 1992, "Direct Sonar Sensing for Mobile Robot Navigation," Kluwer Academic Publishers.

[14] M. A. Fischler and R. C. Bolles, 1981, "Random sample consensus: A paradigm for model fitting with applications to image analysis and automated cartography," Comm. Assoc. Comp. Mach., vol 24(6), pp. 381-395.

[15] S. J. Lee, J. H. Lim, D. W. Cho, C. U. Kang, and W. K. Chung, 2005, "Feature Based Map Building Using Sparse Sonar Data," IEEE/RSJ Intl. Conf. on Intelligent Robots and Systems, pp. 492-496.

[16] S. J. Lee, Y. Lee, J. H. Lim, C. U. Kang, D. W. Cho, W. K. Chung and W. S. Yun, 2006, "Evaluation of Features through Grid Association for Building a Sonar Map," The 2006 IEEE ICRA, pp. 2615-2620.

[17] H. Durrant-Whyte and Tim Bailey, 2006, "Simultaneous Localization and Mapping: Part I," IEEE Robotics & Automation Magazine, pp. 99-180.